

**NASA
Technical
Paper
1948**

December 1981

NASA
TP
1948
c.1

Optimization and Performance Calculation of Dual-Rotation Propellers

Robert E. Davidson

TECH LIBRARY KAFB, NM
0067640

LOAN COPY: RETURN TO
AFWL TECHNICAL LIBRARY
KIRTLAND AFB, N. M.

NASA



**NASA
Technical
Paper
1948**

1981

Optimization and Performance Calculation of Dual-Rotation Propellers

Robert E. Davidson
*Langley Research Center
Hampton, Virginia*

NASA

National Aeronautics
and Space Administration

**Scientific and Technical
Information Branch**

SUMMARY

An analysis is given which enables the design of dual-rotation propellers. It relies on the use of a new tip loss factor deduced from T. Theodorsen's measurements coupled with the general methodology of C. N. H. Lock. The analysis eliminates the possibility of obtaining an infinite chord as would be found by using the tip loss factor advocated by Lock. In addition, it includes the effect of drag in optimizing and does not require the averaging of various quantities across the radius in carrying out off-design calculations. Thus, a combination of the Lock and Theodorsen formulations is described and the possibilities are explored. Some values for the new tip loss factor are calculated for one advance ratio. The calculation is simple and straightforward.

INTRODUCTION

The current interest in fuel-efficient air transportation has given rise to a number of studies aimed at defining the capabilities of large propeller-driven aircraft employing advanced, aerodynamic and engine/propeller concepts. An opportunity for designing more efficient wings and propellers is provided by new design tools which utilize nonlinear transonic-flow codes and improved materials and structural concepts. The development of techniques for achieving more efficient wings has received much attention, particularly in the NASA Aircraft Energy Efficiency (ACEE) Energy Efficient Transport (EET) Program carried out over the past 4 or 5 years. Propeller theory, on the other hand, has been pretty well ignored since the early fifties. Much more research needs to be invested in propeller aerodynamics to bring propeller design up to the level of sophistication achieved by current wing-design methodology.

There are many papers treating both single- and dual-rotation propellers. Analyses pertinent to the present investigation that treat single-rotation propellers can be found in references 1 to 6, and in the references therein. Dual-propeller analyses can be found in references 1, 3, 7, and 8. In references 1 and 7, the problem of minimum induced energy loss is treated at length. Provided in reference 8 is an important treatment of dual-rotation-propeller aerodynamics. A treatment of the calculus of variations that is well suited to establishing Betz' condition (eq. (1.3) in ref. 9) for the optimization of both single- and dual-rotation propellers is given in reference 10.

Overall, it would seem that the theory of single-rotation propellers is slightly more advanced than that for dual-rotation propellers. The theories of Lock and Theodorsen, when applied to dual-rotation propellers, have their shortcomings. For a dual-rotation propeller, any attempt to derive an optimization formula (Betz' condition) based on the Lock formulation of dual-rotation aerodynamics will be found, in practice, to yield a planform which develops infinite chords. The reason is that the tip loss factor used by Lock is only known for single-rotation propellers and is inadequate for dual-rotation propellers. Theodorsen's analysis does not permit the optimization of a dual-rotation propeller with drag considered and, in making off-design calculations, requires the use of the mass coefficient which is averaged over

the radius. The purpose of this paper is to combine the best features of those two methods into a single, modified theory which eliminates the shortcomings just described.

A way has been found to determine Lock's tip loss factor for dual-rotation propellers from Theodorsen's measurements. In order to accomplish this, it was necessary to show that the Theodorsen formulation applies to the setup in which one propeller is behind the other. This new Lock/Theodorsen tip loss factor eliminates the infinite chords and permits an analysis which includes drag and eliminates the need for an averaged quantity. Thus, a combination of Lock's and Theodorsen's formulations is described and the possibilities are explored. Some values for the new tip loss factor are calculated for one advance ratio. The calculation is simple and straightforward.

SYMBOLS

A	abbreviation variable (eqs. (3))
b	equation (B23)
B	number of blades in propeller
c	chord of airfoil
C_D	drag coefficient of blade
C_L	lift coefficient of blade
C_P	power coefficient, $\Omega Q / \rho n^3 d^5$
d	diameter of propeller
dD	drag of blade element
J	advance ratio, V/nd
k	number with same value at all radii to blade sections
$K(x)$	circulation function used by Theodorsen (refs. 1 and 7)
K'	denotes something to be held stationary, in sense of calculus of variations
ℓ	reciprocal of lift-drag ratio
dL	lift of blade element
n	revolutions per second
dP	power loss of blade elements

p', q', r', s' elementary functions of propeller parameters and functions
 (see eq. (16))

dQ torque on blade elements

r radial coordinate

R tip radius

s solidity of either component, $Bc/2\pi r$

t_1 temporary variable (see eq. (7))

u, v components of interference velocity of front propeller on back propeller,
 or vice versa (fig. 1)

V forward speed, or advance velocity (fig. 1)

w trailing helix displacement velocity

\bar{w} = w/V

w_1 interference velocity of either airscrew on itself

W resultant velocity at blade element (fig. 1)

W_0 W for light loading limit (fig. 1)

x = r/R

α angle of attack of two-dimensional airfoil

β total induced angle (see eq. (B9) and fig. 1)

γ self-induced angle (see eqs. (B7) and (B8) and fig. 1)

ζ_{0y} equation (B18)

η efficiency

θ blade angle (no load)

ρ mass density of air

σ product of solidity and lift coefficient, sC_L

ϕ_0 see equations (B9) and (B10) and figure 1

ϕ_{q0} resolving scalar (eq. (9))

χ_0 tip loss factor (see eq. (B1)), $\chi(\phi_0)$

Ω angular velocity

Subscripts:

B back propeller

C mean value for dual-rotation pair

F front propeller

S single propeller

y,z either front airscrew and back airscrew, respectively, or vice versa in equation (B17)

1 induced

2 drag

OPTIMIZATION FORMULA

Betz' condition concerns the effect of making small changes in the chord or the blade angle of a propeller at various radii. It gives a mathematical statement that must hold at each radius when the changes have been made in such a way that the propeller efficiency is highest. For single-rotation propellers, Betz' condition can be derived intuitively as was equation (1.3) in reference 9; however, the more analytical approach of appendix A is preferable, for dual-rotation propellers, especially if the propellers are not assumed to be alike front and back. In this paper, only changes in the chord are considered. The lift coefficient is presumed fixed by airfoil considerations.

The equation by which a dual-rotation propeller can be optimized will now be developed from Betz' condition for dual rotation. This condition is

$$k = \frac{\frac{d}{d\sigma} \left(\frac{dP_F}{dr} + \frac{dP_B}{dr} \right)}{\Omega \frac{d}{d\sigma} \left(\frac{dQ}{dr} \right)} \quad (1)$$

which is equation (A3) in appendix A.

Equation (1) has to be true at any radius r along the blade. In particular, the constant k is to be the same all along the blade. The exact choice of k involves matching the power absorbed by the propeller to the power output of the engine.

The various items in equation (1) will now be selected from appendix B, which gives the appropriate part of Lock's theory. Familiarity with this appendix and with

figure 1 (taken from ref. 8) is assumed. In equation (1), dP_F and dP_B represent both induced dP_1 and airfoil-drag dP_2 power losses. The induced power loss for both propellers is determined by equation (B33):

$$\left(\frac{dP_1}{dr}\right)_C = 2Ab\sigma^2(1 + \chi_0 \cos 2\phi_0) \quad (2)$$

where

$$\left. \begin{aligned} A &= \pi\rho r r^3 \Omega^3 \sec^3 \phi_0 \\ \sigma &= sC_L \\ 1/b &= 4\chi_0 \sin \phi_0 \\ \gamma &= b\sigma \quad (\text{see eq. (B23)}) \end{aligned} \right\} \quad (3)$$

Lock's tip loss factor χ_0 is of primary importance and more will be said about it toward the end of this section. The airfoil-drag power loss for the combination can be similarly written, from equation (B25),

$$\left(\frac{dP_2}{dr}\right)_C = 2A\sigma\ell \quad (4)$$

where

$$\ell = C_D/C_L \quad (5)$$

Adding equations (2) and (4) gives the term to be differentiated in the numerator of equation (1); thus,

$$\left(\frac{dP_F}{dr} + \frac{dP_B}{dr}\right) = 2A\sigma(t_1\sigma + \ell) \quad (6)$$

where

$$t_1 = b(1 + \chi_0 \cos 2\phi_0) \quad (7)$$

The power input to either propeller is given by equation (B26) as

$$\Omega \left(\frac{dQ}{dr}\right) = A \frac{\sigma}{\sec \phi_0} \phi_{q0} \quad (8)$$

where

$$\phi_{q0} = \sin \phi_0 + \ell \cos \phi_0 \quad (9)$$

Equations (6) and (8) are substituted into equation (1) and are differentiated with respect to σ . The result is

$$k = \frac{2(2t_1\sigma + \ell)}{\phi_{q0}/\sec \phi_0} \quad (10)$$

Equation (10) can be solved for σ to obtain

$$\sigma = \frac{\frac{1}{2} k \phi_{q0} \cos \phi_0 - \ell}{2t_1} \quad (11)$$

Substitution of equation (7) into equation (11) yields the optimization formula for the dual-rotation propeller,

$$\sigma = \frac{\frac{1}{2} k \phi_{q0} \cos \phi_0 - \ell}{2 \frac{1}{4 \sin \phi_0} \left(\frac{1}{\chi_0} + \cos^2 \phi_0 - \sin^2 \phi_0 \right)} \quad (12)$$

in which the third of equations (3) was used.

Equation (12) is used to determine the blade-chord distribution once the C_L distribution over r is known. As noted for equation (1), equation (12) has to be true for all values of $r < R$, and in particular, k is the same for all r with a value that has to be found by trial and error to make the power absorbed by the propeller equal to the engine power output. The power absorbed is found by graphically or numerically integrating equation (8) over the radius for both propellers (i.e., the power loss for both propellers is found by multiplying equation (8) by 2). It is helpful to note that the power absorbed should increase with k . Further note that instead of regarding lift coefficient as given, the chord distribution could have been prescribed and then the optimum lift coefficients determined; the airfoils might then be optimized for these lift coefficients. Consider now the function χ_0 .

LOCK'S TIP LOSS FACTOR χ_0

At a given advance ratio J , the function χ_0 is a function of x only. It is the ratio of the induced angle of attack with an infinite number of blades to the induced angle of attack for whatever number of blades happens to be used. Stated another way, it is the average rate of fall of potential, taken around the circle of the blade element, divided by the normal derivative of the potential at the vortex sheet. In view of these physical meanings, it seems obvious that χ_0 must be a significant link between single- and dual-rotation aerodynamics.

It might be thought that the χ_0 for dual-rotation propellers ought to be given a new symbol since the significance seems so different from that in single-rotation propellers. Strangely, however, the new χ_0 is still a single-rotation function because it is merely the χ_0 associated with a single-rotation propeller. This single-rotation propeller, however, does not have the optimum single-rotation propeller loading; it has instead the optimum dual-rotation loading which could be obtained from Theodorsen's circulation function $K(x)$. This radical change in loading makes a considerable difference in the function χ_0 .

Applicability of Theodorsen's Theory to Dual-Rotation Propellers

As pointed out in the Introduction of reference 1, Theodorsen's work was based on the hypothetical situation in which the dual-rotating propellers are operating in the same plane. It was noted that the applicability of Theodorsen's theory to other situations requires further confirmation. This matter will now be considered because it is pertinent to the determination of χ_0 for dual-rotation propellers operating one behind the other on a single axis.

Observe that, when the propellers are in the hypothetical situation of being in the same plane, equations (B32) would be symmetric; thus,

$$\left(\frac{dP_1}{dr}\right)_F = A\sigma\gamma(1 + \chi_0 \cos^2 \phi_0 - \chi_0 \sin^2 \phi_0)$$

$$\left(\frac{dP_1}{dr}\right)_B = A\sigma\gamma(1 + \chi_0 \cos^2 \phi_0 - \chi_0 \sin^2 \phi_0)$$

But, for the combination obtained by adding these two equations, the result would again be equation (B33) in appendix B, with no change in equation (2). Therefore, the previous derivation for the optimizing equation would proceed with no change; equation (12) for σ would be the same whether the two propellers were in the same plane or not. So the optimum planform defined by Theodorsen's theory applies without reservation when the two propellers are mounted one behind the other.

Determination of χ_0 for Dual-Rotation Propellers

The only quantity in equation (12) that cannot be considered known is χ_0 , which first appears in equation (2). The single-rotation values for χ_0 cannot be used, as already noted, but χ_0 for dual-rotation propellers can be determined from a comparison of the Lock and Theodorsen theories.

If the physics and mathematics leading to equation (12) are correct, this equation must produce, with drag neglected, the same results as are obtained from Theodorsen. On page 87 of reference 1 (the equation just before eq. (12)), Crigler gives the following equation for light loadings:

$$sC_L W_0 \equiv \sigma W_0 = \frac{V}{\pi n dx} \bar{w} V K(x)$$

or

$$\sigma = \bar{w} \frac{J}{\pi x} (\sin \phi_0) K(x) \equiv s' \bar{w} \quad (13)$$

On the other hand, equation (12) with drag neglected is

$$\sigma = \frac{\frac{1}{2} k \phi_{q0} \cos \phi_0}{2 \frac{1}{4 \sin \phi_0} \left(\frac{1}{\chi_0} + \cos^2 \phi_0 - \sin^2 \phi_0 \right)} \quad (14)$$

Equating equations (13) and (14) gives

$$k \frac{p'}{q' \left(\frac{1}{\chi_0} + r' \right)} = \bar{w} s' \quad (15)$$

where

$$\left. \begin{aligned} p' &= \frac{1}{2} \phi_{q0} \cos \phi_0 \\ q' &= \frac{2}{4 \sin \phi_0} \\ r' &= \cos^2 \phi_0 - \sin^2 \phi_0 \\ s' &= \frac{J}{\pi x} K(x) \sin \phi_0 \end{aligned} \right\} \quad (16)$$

In the last of equations (16), $K(x)$ comes from the electrical measurements of Theodorsen (fig. 2). Equation (15) can be solved for χ_0 :

$$\chi_0 = \frac{q' s'}{(k/\bar{w}) p' - q' s' r'} \quad (17)$$

An independent derivation has been made of the important equation (17) for determining χ_0 from Theodorsen's electrical measurements. This derivation deals directly with the induced velocities and it is interesting that Betz' condition does not play any part, although it did in the earlier derivation. For details, refer to appendix C.

Everything can be regarded as known in equation (17) except the ratio k/\bar{w} , which will now be found from somewhat tangential considerations. First note that, with drag neglected, the efficiency decrement can be determined by using equations (2) and (8),

$$1 - \eta = \frac{\frac{dP}{dr}}{2\Omega \frac{dQ}{dr}} = \frac{2b(1 + \chi_0 \cos 2\phi_0)\sigma}{2\phi_{q0} \cos \phi_0} = \frac{2t_1\sigma}{2\phi_{q0} \cos \phi_0} \quad (18)$$

If equation (11), with $\ell = 0$, is substituted into equation (18) for σ , there results

$$1 - \eta = \frac{1}{4} k \quad (19)$$

In addition to equation (19), another relation can now be found between η and \bar{w} . In figure 3 (which is taken from ref. 1), η is seen to be practically linear with \bar{w} for light loadings. The slope $d\eta/d\bar{w}$ is taken to be

$$\frac{d\eta}{d\bar{w}} = -0.5 \quad (20)$$

which means that

$$1 - \eta = -\frac{d\eta}{d\bar{w}} \bar{w} = 0.5\bar{w} \quad (21)$$

Therefore, from equations (19) and (21), it follows that

$$\left. \begin{array}{l} 0.5\bar{w} = \frac{1}{4} k \\ \text{or} \\ \frac{k}{\bar{w}} = 2.0 \end{array} \right\} \quad (22)$$

With this result, everything is known in equation (17).

The tip loss factor χ_0 defined by Lock can now be calculated from the electrical measurements of Theodorsen (refs. 1 and 7) by using equation (17). Some numerical values have been calculated and are discussed in "Results" and in appendix D.

Limiting Forms of χ_0

The behavior of χ_0 near $x = 0$ and 1 will now be investigated.

$x = 0$. - It can be seen that $p' = 0$ and $r' = -1$, since $\phi_0 = \pi/2$; and $q' = 1/2$, while $s' \rightarrow \infty$ (see eq. (16)). Therefore, equation (17) shows $\chi_0 = 1$ at $x = 0$. This is as it should be, since $\chi_0 = 1$ would be true in the vicinity of a vortex on the axis; this vortex is a feature of the optimum dual-rotation propeller.

$x = 1$. - The functions p' , q' , and r' are all finite (see eq. (16)); but $s' = 0$ at $x = 1$ because $K(x)$ is zero there. Equation (17) now shows clearly that $\chi_0 = 0$ at $x = 1$. This is as it should be from the definition of χ_0 .

All the equations necessary for the optimization of a dual-rotation propeller, with drag considered, have now been obtained. But for complete definition of the propeller (i.e., to specify the blade-angle distributions, front and back, in addition to the chord distribution), the equations for the induced angle of attack β_y are needed. These equations are picked out of appendix B and given explicitly in the section "Dual-Rotation Propeller Calculations," where they are also needed for other purposes, like performance calculations.

Recapitulation

In the optimization equation (eq. (12)), everything on the right may be regarded as something given, except χ_0 , which is found from equation (17). In using equation (17), equation (22) has to be used. It was encouraging to find that Theodorsen's work could be applicable to the setup where one propeller is behind the other. It would be possible to determine χ_0 for all possible dual-rotation propellers, beforehand, using equation (17); then, in this sense, everything on the right in equation (12) would be known.

DUAL-ROTATION PROPELLER CALCULATIONS

Optimum Propeller

In order to calculate the optimum chord distribution, it is only necessary to be given the values of J and C_p and the "airfoil data." The "airfoil data" are actually preselected in the sense that the airfoil and the value of C_L , C_D , or α have been preselected to produce a desirable condition, like $(C_L/C_D)_{\max}$, at each radial station along the wing. Then, σ can be calculated from equation (12) using χ_0 obtained by the procedure given in appendix D.

If the airfoil data are limited and therefore erratic, this will be reflected in the shape of the blade planform. This could cause the blade to be unacceptably erratic, requiring smoothing and implying a questionable smoothing of airfoil data. The sensitivity of the airfoil sections to Mach number and Reynolds number may restrict the operating range of altitude and flight velocity at which the propeller will be optimum. For instance, an operating condition could be envisioned in which the airfoils are supposed to be supercritical over much or all of the blade so that the planform might take a very special shape.

The no-load blade angle is given by

$$\theta_Y + (\text{Torsional deflection}) = \phi_0 + \beta_Y + \alpha \quad (23)$$

in which the total induced angle β_Y is given by equation (B27) (taking account of eq. (B31)) so that

$$\beta_Y = \gamma(1 + \zeta_{0Y}) \quad (24)$$

and further, from equation (B23),

$$\beta_Y = b\sigma(1 + \zeta_{0Y}) \quad (25)$$

The ζ_{0Y} are defined by the equations immediately following equation (B28); thus,

$$\left. \begin{aligned} \zeta_{0F} &= \chi_0 \cos^2 \phi_0 \\ \zeta_{0F} &= \chi_0 (\cos^2 \phi_0 - 2 \sin^2 \phi_0) \end{aligned} \right\} \quad (26)$$

Then equation (25) can be written out, for use in equation (23), as

$$\left. \begin{aligned} \beta_F &= b\sigma(1 + \zeta_{0F}) \\ \beta_B &= b\sigma(1 + \zeta_{0B}) \end{aligned} \right\} \quad (27)$$

Note that equations (27) do not depend on any averaged quantities like the "mass coefficient" (compare with p. 86 in ref. 1, relative to interference velocities).

The detailed procedure for optimization is given in appendix E.

Nonoptimum Propeller, Given Propeller, Off-Design Conditions

Mathematically, these problems involve replacing equation (12) by equation (23). The resulting system, comprising equation (23), two new induced angle-of-attack formulas in place of equations (27), and the two-dimensional airfoil data (which may come from either wind-tunnel test or from airfoil theory) are to be solved by iteration, perhaps starting with the assumption that the β_Y are zero. Then, an initial α_Y can be calculated from equation (23) and a starting C_{Ly} is taken from airfoil data. Next, an initial β_Y can be found which yields new values of α_Y and C_{Ly} and establishes an iteration loop.

A new formula for β_y is needed because the C_{Ly} are no longer the same front and back (although s is). From equation (B27) it is seen that the formulas (27) for β_y now become

$$\beta_y = bs(C_{Ly} + \zeta_{0y}C_{Lz})$$

or

$$\left. \begin{aligned} \beta_F &= bs(C_{LF} + \zeta_{0F}C_{LB}) \\ \beta_B &= bs(C_{LB} + \zeta_{0B}C_{LF}) \end{aligned} \right\} \quad (28)$$

A new form of equation (23) should be added to these equations because now α_y are not the same front and back:

$$\theta_y + (\text{Torsional deflection}) = \phi_0 + \beta_y + \alpha_y \quad (29)$$

This equation is usually very sensitive because θ_y and ϕ_0 are often nearly the same. In particular, the torsional deflection may be considerable.

The nonoptimum propeller calculation is not simple because it is iterative and requires the storage of airfoil data. There is also a more fundamental difficulty: the circulation function has only been determined for the Theodorsen optimum propeller. The more the propeller and/or operating condition departs from Theodorsen's optimum, the more questionable this calculation is. However, experience with single-rotation propellers indicates that the results of this calculation will hold surprisingly well.

A more rigorous, but clearly more difficult, method would include arbitrary propeller theory in the loop (as given in refs. 2 and 4). Then, each time a circulation distribution is obtained, a rigorous induced velocity and β_y would be found. This simpler procedure should be of great value in getting started and often may be sufficient without the introduction of arbitrary propeller theory.

Lock's methodology (ref. 8) appears to make calculations for dual-rotation propellers essentially like those for single-rotation propellers.

See appendix F for detailed procedure of nonoptimum propeller calculations.

RESULTS

The function χ_0 has been calculated for dual-rotation propellers, with $J = 5.1693$ at several values of x , by using the procedure outlined in appendix D. There were four blades front and four back.

The calculated values of χ_0 are shown in figure 4 plotted against x . Also shown is the corresponding curve for single-rotation propellers. The curves are seen to differ considerably. Note that since $\sin \phi_0$ is a function only of x at a given J , χ_0 can also be plotted against $\sin \phi_0$ as in figure 5.

Shown in figure 5 (fig. 5 of ref. 6) are the conventional contours of χ_0 for single-rotation propellers. The arrows show how the base points (single rotation) are shifted for dual rotation. The arrow points and the base points are calculated for the same value of J ; hence, the shift is vertical. Observe that by performing the calculation of χ_0 at a sufficient number of values of J , a new set of curves can be mapped like the ones for single-rotation propellers.

DISCUSSION

The paper is now largely complete. Some isolated topics will now be taken up in the light of what has been said in previous sections.

Question of Infinite Chords

If equations (16) and (17) are substituted in equation (12) with $\ell = 0$, there results

$$\sigma = \frac{k}{k/\bar{w}} \frac{J}{\pi x} \sin \phi_0 K(x) \quad (30)$$

but, since

$$\sigma \equiv sC_L$$

and

$$s \equiv \frac{B(c/d)}{\pi x}$$

it follows that

$$\frac{c}{d} = \frac{1}{BC_L} \frac{k}{k/\bar{w}} J K(x) \sin \phi_0 \quad (31)$$

Since all quantities on the right of equation (31) are finite, it is clear that c/d is finite. There can be no infinite chords when χ_0 is determined in the way given in this paper.

Competition Between Single and Dual Rotation

The equations given herein degenerate easily into single rotation without change in form. It is only necessary to see that any term involving ζ_{0y} is to be removed.

The optimization of single- or dual-rotation propellers is a simple calculation; therefore, the safest and best method of evaluating single- and dual-rotation propellers would seem to be a simple comparison of various complete propeller optimizations as to efficiency, weight, and cost, rather than an attempt to discern trends in the equations. Cost might be set proportional to the total number of blades. Weight might be strongly influenced by J , but it is not too clear because the propellers turn slower with increased J and centrifugal stresses are relieved.

In particular, the two curves in figure 4 labeled "single" and "dual" tell nothing of the relative merit of single and dual rotation, because they are both for the same advance ratio and the total number of blades for the single-rotation propeller is only half that for the dual-rotation propeller. The single-rotation propeller is likely to have twice the number of blades as either of the dual-rotation pair and the values of J might differ considerably.

Comparison of χ_0 for Single and Dual Rotation

The most characteristic difference between the two kinds of χ_0 is that the values for single rotation greatly exceed unity for inboard radii while the values for dual rotation stay below unity or exceed it only slightly. The reason for this difference is that $\chi_0 = 1$ marks the radius where, for a high- J propeller, the benefit from dual rotation completely cancels self-induced losses.

This cancellation can be seen in the equations for the induced power loss and the induced angle of attack. The axial losses do not participate in the dual-rotation action and tend to make the cancellation less clear so that, for simplicity, the propeller of very high J will be considered. Now, $\phi_0 \rightarrow \pi/2$ and $\cos 2\phi_0 \rightarrow -1$; therefore, equation (2) for the induced power loss becomes

$$\left(\frac{dP_1}{dr}\right)_C = A2b\sigma^2(1 - \chi_0)$$

which shows that the induced power loss becomes negative when χ_0 exceeds unity. Clearly, the optimized chords will become large where $\chi_0 = 1$. Any optimization process must have built-in controls for preventing the catastrophe of infinite chords at $\chi_0 = 1$. Theodorsen's electrical-analogy approach bridged all this mathematical difficulty and went directly to the ultimate solution.

These matters can be seen again in equations (26) and (27) for the induced angle of attack. There it is seen that the place on the blade where $\chi_0 = 1$ is where the sum of the induced angles of attack of front and back propellers is zero. Again, these remarks apply to the very-high- J propeller where the beclouding effect of the axial losses is absent.

Compromised Optimum Propeller

It seems inevitable that the optimum dual-rotation propeller will be compromised because of the awkwardly large inboard chords. In other words, the chords inboard may be arbitrarily reduced for a practical reason, like a prohibitively great length of propeller shaft needed to accommodate the large inboard chords.

Furthermore, it is true that the efficiency is not very sensitive to variations of the planform from the optimum, as in wings where the straight-tapered planform is almost as good as the elliptical planform. So, why is the optimum given so much attention in the literature? Perhaps the answer is that the optimum serves as a reference by which compromises can be kept under control. Thus, most of the work of aerodynamic optimization may be done from the standpoint of the given propeller (app. F) with relatively little attention given to the optimum propeller (app. E).

The function χ_0 is indispensable in calculating the performance of the given propeller (app. F), yet it is determined from measurements for the optimum propeller. It is somewhat paradoxical to use off-design calculations to optimize a propeller when these off-design calculations make use of a χ_0 determined from optimum propeller results. The point is single-rotation experience indicates χ_0 can be "stretched" to provide answers that are useful in off-design conditions, although this may not extend as well to dual-rotation propellers.

CONCLUSIONS

The Theodorsen and Lock treatments of dual-rotation propellers were combined, and it is possible to draw the following conclusions:

1. The function χ_0 , tip loss factor, used in the Lock treatment can be determined for dual-rotation propellers from Theodorsen's electrical analogy. Formerly, these functions only existed for single rotation and were inadequate for dual rotation.
2. The effect of airfoil drag can be included in the optimization of dual-rotation propellers.
3. Combination of the Lock and Theodorsen treatments enables the off-design performance of dual-rotation propellers to be estimated without reliance on an averaged quantity, such as the mass coefficient advanced by Theodorsen. The mass coefficient has only one value for the whole propeller disc.
4. Conclusion 3 also applies to the calculation of the blade angles of optimum dual-rotation propellers.
5. From the Lock treatment of dual-rotation propellers, it can be shown that the optimum planform is the same whether the two propellers are in the same plane or one behind the other.
6. The combination of the Lock and Theodorsen theories appears to enhance both of those works.

Langley Research Center
National Aeronautics and Space Administration
Hampton, VA 23665
November 23, 1981

APPENDIX A

CALCULUS OF VARIATIONS APPROACH TO MAXIMUM EFFICIENCY

The quantity that is to be minimized is the total power loss for both propellers

$$\int_0^R \left(\frac{dP_F}{dr} + \frac{dP_B}{dr} \right) dr$$

The quantities that are held constant in the process are the power absorbed for both propellers,

$$\int_0^R \Omega \frac{dQ_F}{dr} dr \quad \text{and} \quad \int_0^R \Omega \frac{dQ_B}{dr} dr$$

The latter two are not summed. They are held constant individually, but it is not stated at this point what these constants are. The chords, and hence σ , are not yet assumed to be the same front and back.

Chapter 6 of reference 10 will be followed with particular emphasis on sections 6.2 and 6.5. In these sections, there is unfortunate, but probably necessary, rotation of the meanings of symbols. The independent variable σ becomes y and the dependent variable r becomes x , in paragraph 6.5. But in paragraph 6.2, x and y represent dependent variables like σ , and t represents the independent variable.

For K' (in ref. 10 K is not primed),

$$K' = \left(\frac{dP_F}{dr} + \frac{dP_B}{dr} \right) + k_F \Omega \frac{dQ_F}{dr} + k_B \Omega \frac{dQ_B}{dr} \quad (A1)$$

in which the dP and dQ depend on σ .

Then for Euler's equation (eq. (6-15)) in the reference,

$$\frac{\partial K'}{\partial \sigma} - \frac{d}{dt} \frac{\partial K'}{\partial \sigma_r} = 0$$

There is no σ_r in this problem, so the second term is zero. The Euler equation becomes

$$\frac{\partial K'}{\partial \sigma} = 0$$

APPENDIX A

Since there are two σ 's (σ_F and σ_B), there are two Euler equations. Thus,

$$\frac{\partial K'}{\partial \sigma_F} = 0$$

and

$$\frac{\partial K'}{\partial \sigma_B} = 0$$

Now the sum of the power losses depends on both σ_F and σ_B , but the power absorbed by the front propeller does not depend on σ_B and vice versa. The two Euler equations then become

$$\left. \begin{aligned} \frac{\partial}{\partial \sigma_F} \left(\frac{dP_F}{dr} + \frac{dP_B}{dr} \right) + k_F \Omega \frac{\partial}{\partial \sigma_F} \left(\frac{dQ_F}{dr} \right) = 0 \\ \frac{\partial}{\partial \sigma_B} \left(\frac{dP_F}{dr} + \frac{dP_B}{dr} \right) + k_B \Omega \frac{\partial}{\partial \sigma_B} \left(\frac{dQ_B}{dr} \right) = 0 \end{aligned} \right\} \quad (A2)$$

In these equations, the dP and dQ are taken from appendix B, then equations (A2) are two relations defining σ_F and σ_B as functions of r . When σ is the same front and back as in the text, the two equations become one (Q_F and Q_B are the same when $\sigma_F = \sigma_B$ in the approximation accepted). Then equations (A2) become

$$\frac{d}{d\sigma} \left(\frac{dP_F}{dr} + \frac{dP_B}{dr} \right) + k\Omega \frac{d}{d\sigma} \left(\frac{dQ}{dr} \right) = 0 \quad (A3)$$

which, except for the nonessential sign of k , is the same as equation (1) in the text and is the desired Betz condition.

APPENDIX B

INTERFERENCE VELOCITY FOR A CLOSE PAIR
OF CONTRA-ROTATING AIRSCREWS

by

C. N. H. Lock

The British Crown holds the copyright for the report, R & M No. 2084, which is reproduced in this appendix with permission of the Controller of Her Britannic Majesty's Stationery Office.

Interference Velocity for a Close Pair of Contra-rotating Airscrews

By

C. N. H. Lock, M.A., F.R.Ae.S.,
of the Aerodynamics Division, N.P.L.

Reports and Memoranda No. 2084

22nd July 1941

Summary.—A method is developed of calculating the performance of a pair of contra-rotating airscrews, closely analogous to that described in R. & M. 2035³ for a single airscrew. The assumptions made are considered to be theoretically justifiable if the interference velocities are so small that their squares and products may be neglected. It is hoped to compare calculations by the present method with experimental results.

The equations have been applied by an approximate single radius method to give the difference in blade setting between the front and back airscrews for equal power input; a comparison is also made between the efficiencies of single- and contra-rotating airscrews.

1. *Introduction.*—The present note contains equations for a close contra-rotating pair of airscrews based on the same assumptions as those of R. & M. 1674¹ and 1849², together with the following special assumptions. These assumptions appear to be justifiable when the interference velocities are considered as small quantities of the first order of which squares and products may be neglected.

(i) The interference velocities at any blade element may be calculated by considering the velocity fields of the two airscrews independently and adding the effects.

(ii) Either airscrew produces its own interference velocity field which so far as it affects the airscrew itself is exactly the same as if the other airscrew were absent and includes the usual tip loss correction.

(iii) Added to this is the velocity field of the other airscrew. Since the two are rotating in opposite directions, the effect will be periodic and its time average value may be taken to be equal to the average value round a circle having a radius of the blade element.

(iv) In considering the interference of either airscrew on the other, it is necessary to resolve the mean interference velocity into axial and rotational components.

The average value round a circle of the axial component interference velocity varies slowly through the airscrew disc. It is therefore reasonable to assume for the axial component for a *close* contra-rotating pair that the effect of either airscrew (y) on the other (z) is equal to the mean axial component in the plane of the airscrew disc of (y).*

The average value round a circle of the rotational component is zero³ at any distance in front of the airscrew disc and has a constant value at any distance behind, this value being twice the mean effective value for the airscrew blade sections. It is therefore assumed as regards the rotational component that the effect of the rear airscrew on the forward airscrew is zero; the effect of the forward airscrew on the rear airscrew is equal to twice the mean value of the rotational component in the plane of the disc of the forward airscrew with its direction reversed.

* Varying degrees of closeness might be allowed for empirically by multiplying u_r by $(1 - \mu)$ and u_b by $(1 + \mu)$, where μ is a parameter varying from a small value for a close pair to a value near unity for a distant pair.

3

For the thrust and torque acting on a blade element we have the usual equations

$$dT = N(dL \cos \phi - dD \sin \phi),$$

$$(1/r)dQ = N(dL \sin \phi + dD \cos \phi),$$

where

$$dL = \frac{1}{2}\rho c W^2 C_L dr,$$

$$dD = \frac{1}{2}\rho c W^2 C_D dr,$$

so that

$$(dT/dr) = \pi \rho r s W^2 (C_L \cos \phi - C_D \sin \phi), \quad \dots \dots \dots (13)$$

$$(1/r)(dQ/dr) = \pi \rho r s W^2 (C_L \sin \phi + C_D \cos \phi). \quad \dots \dots \dots (14)$$

For the total power loss (power input minus thrust power) we have

$$\Omega dQ - V dT = NdL (r\Omega \sin \phi - V \cos \phi) + NdD (r\Omega \cos \phi + V \sin \phi).$$

By the geometry of Fig. 1 it follows that for the induced loss (defined here as the part of the power loss depending on the lift of the blade elements),

$$dP_1 \equiv NdL (r\Omega \sin \phi - V \cos \phi),$$

$$(dP_1/dr) = \pi \rho r s W^2 r \Omega \sec \phi_0 C_L \sin \beta, \quad \dots \dots \dots (15)$$

and for the drag loss

$$dP_2 \equiv NdD (r\Omega \cos \phi + V \sin \phi),$$

$$(dP_2/dr) = \pi \rho r s W^2 r \Omega \sec \phi_0 C_D \cos \beta. \quad \dots \dots \dots (16)$$

Equations (13-16) are all identical in form with those for a single airscrew.

Equations (10-16) with (3-6) will be developed into forms analogous to those of R. & M. 1849² and R. & M. 1674¹ in §7 and §8 respectively. The most practical and useful form is obtained by considering β and γ as small quantities and neglecting squares and products of β and γ for both airscrews. The resulting equations analogous to those of R. & M. 2035³ are developed in §§3-5.

3. *First Order Theory.*—Consider β, γ as small quantities of the first order and write

$$\left. \begin{aligned} u_y &= \mu_{0y} w_{1z}, \\ v_y &= \nu_{0y} w_{1z}, \end{aligned} \right\} \dots \dots \dots (17)$$

and

$$\left. \begin{aligned} \mu_{0y} \sin \phi_{0y} - \nu_{0y} \cos \phi_{0y} &= \xi_{0y}, \\ \mu_{0y} \cos \phi_{0y} + \nu_{0y} \sin \phi_{0y} &= \zeta_{0y}, \end{aligned} \right\} \dots \dots \dots (18)$$

where either $y = F, z = B$ or $y = B, z = F$.

Thus equation (11) gives for either airscrew,

$$W_y = r\Omega_y \sec \phi_{0y} + \xi_{0y} W_{yz} + O(\gamma^2), \quad \dots \dots \dots (19)$$

and substitution in equation (12) gives

$$(\beta - \gamma) r \Omega_y \sec \phi_{0y} = \zeta_{0y} r \Omega_z \sec \phi_{0z} + O(\gamma^2), \quad \dots \dots \dots (20)$$

for either $y = F, z = B$ or $y = B, z = F$. On the basis of equations (3-6) we have,

$$\left. \begin{aligned} \mu_{0F} &= \mu_{0B} \cos \phi_{0B} + O(\gamma), \\ \nu_{0F} &= O(\gamma), \\ \mu_{0B} &= \mu_{0F} \cos \phi_{0F} + O(\gamma), \\ \nu_{0B} &= -2\mu_{0F} \sin \phi_{0F} + O(\gamma). \end{aligned} \right\} \dots \dots \dots (21)$$

For the combination of two airscrews

$$(dP_1/dr)_c = \pi\rho\gamma (\gamma\Omega \sec \phi_0)^2 2sC_L\gamma (1 + \kappa_0 \cos 2\phi_0) + O(\gamma^3) \quad \dots \quad (33)$$

Equations (31–33) and (25) transformed into equations for the coefficient p_{C1} , p_{C2} of induced drag power loss, analogous to equations (31) and (33) of R. & M. 2035³, may be used to calculate the power loss grading for all radii for a given distribution of sC_L (equal for the two airscrews); the corresponding blade angle distribution may be obtained from §5. The power input grading (torque grading) may be obtained from equation (26) or more accurately (as in R. & M. 2035³) from equation (14) using the more accurate value of W obtained below in §6. In the latter case the power input will not be exactly equal for the two airscrews if the values of sC_L are equal. The second order difference in sC_L required to make the power inputs equal to the second order is determined in §6. Or, the performance for a given blade angle distribution may be deduced from the equations of §5; the blade angles at standard radius (0.7) might be adjusted to give equal power input at that radius.

Example.—For the purpose of illustration equations (33), (25) and (26) have been used to calculate the partial efficiency for a section at standard radius (0.7) for equal rotational speed and power input. The formulae (deducible from equations (31–33), (25) and (26)) are

$$1 - \eta_F = \frac{\gamma C_L (1 + \kappa_0 \cos^2 \phi_0) + C_D}{\cos \phi_0 (C_L \sin \phi_0 + C_D \cos \phi_0)}, \quad \dots \quad (34)$$

$$1 - \eta_B = \frac{\gamma C_L (1 + \kappa_0 \cos^2 \phi_0 - 2\kappa_0 \sin^2 \phi_0) + C_D}{\cos \phi_0 (C_L \sin \phi_0 + C_D \cos \phi_0)}, \quad \dots \quad (35)$$

$$1 - \eta_C = \frac{\gamma C_L (1 + \kappa_0 \cos 2\phi_0) + C_D}{\cos \phi_0 (C_L \sin \phi_0 + C_D \cos \phi_0)}, \quad \dots \quad (36)$$

with

$$\gamma = sC_L/(4\kappa_0 \sin \phi_0) = bsC_L \quad \dots \quad (37)$$

In Fig. 2 values of $(1 - \eta_C)$ are plotted for a range of values of J for (1) a pair of contra-rotating two bladers and (2) a pair of contra-rotating three-bladers and for the following values of s , C_L and C_D :—

$$s = 0.090, \quad C_L = 0.56, \quad C_D = 0.017.$$

The values of s and C_L are those at radius 0.7 for airscrew *B* in R. & M. 2021⁴, while the value of C_D is adjusted to give a partial efficiency for this radius equal to the calculated efficiency (0.878) for the whole airscrew. The calculations correspond therefore, to a power input to each airscrew of 2,000 h.p. at 450 m.p.h. equal to that assumed in R. & M. 2021⁴ (a total of 4,000 h.p. for the two airscrews) for the same diameter, rotational speed and height. They were made for a range of values of J from 1.27 to 4.54.* They are compared with the corresponding efficiency figures for a single airscrew of double (the same total) number of blades and solidity and also with airscrews having the same number of blades as one of the contra-rotating pairs and the same total solidity. The equation corresponding to (36) for a single airscrew is

$$1 - \eta_s = \frac{\gamma C_L + C_D}{\cos \phi_0 (C_L \sin \phi_0 + C_D \cos \phi_0)} \quad \dots \quad (38)$$

with (37) in which it must be remembered that values of κ_0 and s must be used, appropriate to the *total* number of blades and solidity. Thus the value of s for the single propeller has twice the value for the corresponding contra-rotating pair, and so the value of γ in (38) would be double that in (36) apart from the change in κ_0 due to doubling the number of blades.

The results of Fig. 2 show that for the present case the increase of efficiency as between the 2-bladers (contra-rotating) and the 4-bladers (single-rotating) varies from 1.0 per cent. to 4.6 per cent., and the increase as between the 3-bladers (contra-rotating) and the 6-bladers (single-rotating) varies from 1.7 per cent. to 4.8 per cent. for the particular values of s , C_L and C_D chosen.

* The actual efficiency figures for the highest values of J would in practice be reduced by the increase of C_D due to increased compressibility effect.

6. *Values of W and $\Omega(dQ/dr)$ to the Second Order in γ .*—The value of W to the second order can be obtained from equation (11) in the form

$$\begin{aligned} W_y &= r\Omega_y \sec \phi_{0y} + \xi_{0y} r \Omega_x \sec \phi_{0x} \gamma_x \\ &= r\Omega_y \sec \phi_{0y} \{1 + \xi_{0y} \lambda_{yx} \gamma_x\} + O(\gamma^2) . \quad \dots \dots \dots (49) \end{aligned}$$

The expressions for dT/dr and dQ/dr involve the factors $\sin \phi$, $\cos \phi$ which may be written,

$$\sin \phi = \sin \phi_0 (1 + \beta \cot \phi_0) + O(\gamma^2) , \quad \dots \dots \dots (50)$$

$$\cos \phi = \cos \phi_0 (1 - \beta \tan \phi_0) + O(\gamma^2) , \quad \dots \dots \dots (51)$$

with

$$\beta_y = \gamma_y + \zeta_{0y} \lambda_{yx} \gamma_x + O(\gamma^2) , \quad \dots \dots \dots (52)$$

from (22). Equation (49) then gives

$$\begin{aligned} W_y^2 \sin \phi_y &= r^2 \Omega_y^2 \tan \phi_{0y} \sec \phi_{0y} \{1 + [2\xi_{0y} + \zeta_{0y} \cot \phi_{0y}] \lambda_{yx} \gamma_x \\ &\quad + \gamma_y \cot \phi_{0y}\} + O(\gamma^2) , \quad \dots \dots (53) \end{aligned}$$

$$W_y^2 \cos \phi_y = r^2 \Omega_y^2 \sec \phi_{0y} \{1 + [2\xi_{0y} - \zeta_{0y} \tan \phi_{0y}] \lambda_{yx} \gamma_x - \gamma_y \tan \phi_{0y}\} + O(\gamma^2) ; \quad \dots (54)$$

or

$$\begin{aligned} W_y^2 \sin \phi_y &= r^2 \Omega_y^2 \sec^2 \phi_{0y} \{\sin \phi_{0y} + \frac{1}{2} \lambda_{yx} \gamma_x [\mu_{0y} (3 - \cos 2\phi_{0y}) - \nu_{0y} \sin 2\phi_{0y}] \\ &\quad + \gamma_y \cos \phi_{0y}\} + O(\gamma^2) , \quad \dots \dots (55) \end{aligned}$$

$$\begin{aligned} W_y^2 \cos \phi_y &= r^2 \Omega_y^2 \sec^2 \phi_{0y} \{\cos \phi_{0y} + \frac{1}{2} \lambda_{yx} \gamma_x [\mu_{0y} \sin 2\phi_{0y} - \nu_{0y} (3 + \cos 2\phi_{0y})] \\ &\quad - \gamma_y \sin \phi_{0y}\} + O(\gamma^2) . \quad \dots \dots (56) \end{aligned}$$

In evaluating $\Omega(dQ/dr)$ and $V(dT/dr)$ it is reasonable to consider C_D/C_L , as before, as a small quantity of the same order as γ , and to write

$$\Omega(dQ/dr) = \pi \rho r^2 \Omega W^2 \sin \phi sC_L \{1 + (C_D/C_L) \cot \phi_0\} + O(\gamma^3) , \quad \dots \dots (57)$$

$$V(dT/dr) = \pi \rho r^2 \Omega \tan \phi_0 W^2 \cos \phi sC_L \{1 - (C_D/C_L) \tan \phi_0\} + O(\gamma^3) . \quad \dots \dots (58)$$

In these expressions $W^2 \sin \phi$, $W^2 \cos \phi$, are given by equations (53–56) in which γ is given by

$$\gamma = bsC_L,$$

so that the torque and thrust power loss grading may be evaluated as far as terms of order γ^2 if the value of sC_L is known to this order for each airscrew. Equations (43–46) give the values of sC_L for each airscrew in terms of the blade angle settings.

Strictly speaking, equations (23) and (40) are only correct to the first order in γ and α , but it was suggested in R. & M. 2035³ that in practice the curves of C_L against α in the unstalled range and of sC_L against γ over a considerable range of large values of J , are straight lines to a higher order of approximation. The additional order of accuracy would then apply to equations (43) since they are deducible from (23) and (40) by linear transformations; the values of sC_L deduced from (43) for given blade angles would then be sufficiently accurate when substituted in (57) and (58) to give values of thrust and torque power correct as far as terms in γ^2 . In any case the value of power loss given by taking the difference between power input deduced from (57) and useful power deduced from (58), will be consistent with (24) and (25) and correct to the same order as the latter equations.

8

Case of Equal Revolutions to Second Order.—Substitution of

$$\mu_{0F} = \mu_{0B} = \kappa_0 \cos \phi_0 ,$$

$$v_{0F} = 0 ,$$

$$v_{0B} = - 2\kappa_0 \sin \phi_0$$

in (53–56), gives

$$W_F^2 \sin \phi_F = r^2 \Omega^2 \tan \phi_0 \sec \phi_0 \{1 + \gamma_F \cot \phi_0 + \kappa_0 \gamma_B (\cot \phi_0 + \sin \phi_0 \cos \phi_0)\} + O(\gamma^2) , \quad \dots \quad (59)$$

$$W_B^2 \sin \phi_B = r^2 \Omega^2 \tan \phi_0 \sec \phi_0 \{1 + \gamma_B \cot \phi_0 + \kappa_0 \gamma_F (\cot \phi_0 + 3 \sin \phi_0 \cos \phi_0)\} + O(\gamma^2) , \quad \dots \quad (60)$$

$$W_F^2 \cos \phi_F = r^2 \Omega^2 \sec \phi_0 \{1 - \gamma_F \tan \phi_0 + \kappa_0 \gamma_B \sin \phi_0 \cos \phi_0\} + O(\gamma^2) , \quad \dots \quad (61)$$

$$W_B^2 \cos \phi_B = r^2 \Omega^2 \sec \phi_0 \{1 - \gamma_B \tan \phi_0 + \kappa_0 \gamma_F (2 \tan \phi_0 + 3 \sin \phi_0 \cos \phi_0)\} + O(\gamma^2) . \quad (62)$$

Equal Power Input to Second Order.—It is evident that the difference $C_{LF} - C_{LB}$ will be of order γ^2 and it is therefore reasonable to assume that $C_{DF} - C_{DB}$ is of order γ^3 . The condition of equal power input will therefore be taken as

$$(sC_L W^2 \sin \phi)_F = (sC_L W^2 \sin \phi)_B + O(\gamma^3) . \quad \dots \quad (63)$$

Condition (63) may be satisfied by writing $\gamma_F = \gamma_B = \gamma$ in (59–62), since this is true to the first order, and putting

$$(sC_L)_F = sC_L (1 + \kappa_0 \gamma \sin \phi_0 \cos \phi_0) , \quad \dots \quad (64)$$

$$(sC_L)_B = sC_L (1 - \kappa_0 \gamma \sin \phi_0 \cos \phi_0) \quad \dots \quad (65)$$

in (63), where sC_L is a mean value between the two airscrews. The final expressions for the thrust and torque grading will be for either airscrew,

$$\Omega(dQ/dr) = \pi \rho r^4 \Omega^3 \tan \phi_0 \sec \phi_0 \{sC_L \{1 + \gamma [\cot \phi_0 + \kappa_0 (\cot \phi_0 + 2 \sin \phi_0 \cos \phi_0)]\} + sC_D \cot \phi_0\} ; \quad \dots \quad (66)$$

and for the front and back airscrews separately,

$$V(dT/dr)_F = \pi \rho r^4 \Omega^3 \tan \phi_0 \sec \phi_0 \{sC_L \{1 + \gamma [- \tan \phi_0 + 2\kappa_0 \sin \phi_0 \cos \phi_0]\} - sC_D \tan \phi_0\} , \quad \dots \quad (67)$$

$$V(dT/dr)_B = \pi \rho r^4 \Omega^3 \tan \phi_0 \sec \phi_0 \{sC_L \{1 + \gamma [- \tan \phi_0 + 2\kappa_0 (\tan \phi_0 + \sin \phi_0 \cos \phi_0)]\} - sC_D \tan \phi_0\} . \quad (68)$$

The difference between these expressions for torque and thrust power agrees with the first order value of power loss given in (31–33). Expressions for the blade angle to the second order could be deduced from §7, equation (76) below, but would be rather complicated.

7. *Exact Transformation of Equations (11) and (12) into a Form Analogous to the Equations of R. & M. 1849².*—Write

$$\left. \begin{aligned} u_y &= \mu_y w_{1z} , \\ v_y &= \nu_y w_{1z} , \end{aligned} \right\} \quad \dots \quad (69)$$

where either $y = F, z = B$, or $y = B, z = F$, and μ_y, ν_y are functions of ϕ_y, ϕ_z (according to equations (3–6), of ϕ_z only).

Write

$$\left. \begin{aligned} \mu \sin \phi - \nu \cos \phi &= \xi , \\ \mu \cos \phi + \nu \sin \phi &= \zeta . \end{aligned} \right\} \quad \dots \quad (70)$$

§5. This section gives first order results for given blade angles and also the first order difference of blade angle between front and back airscrews for the case of equal angular velocity and power input. This completes the formulae necessary to obtain the numerical results given in the present note.

§6. Values of W , (dQ/dr) and (dT/dr) are given to the second order for known values of C_L . Difference of C_L between the two airscrews is determined to the second order for equal revolutions and power input. The resulting value of the difference between the thrust power and torque power checks with the first order estimation of power loss in §3.

§7. In this section equations are obtained analogous to those on which the charts of R. & M. 1849² are based.

§8. In this section equations analogous to those of R. & M. 1674¹ are developed which could be used in the absence of charts to calculate the exact performance of an airscrew on the basis of assumption (i)-(iv).

LIST OF SYMBOLS

- a Reciprocal of slope of lift curve. Equation (40).
- b Equation (23).
- B suffix For "back airscrew".
- c Blade chord.
- C suffix Mean value for contra-rotating pair of airscrews.
- C, D Equation (71).
- C_L, C_D Lift and drag coefficients of blade element.
- dD Drag of blade element.
- F suffix For "front airscrew".
- $J = \pi V/R\Omega$.
- dL Lift of blade element.
- N Number of blades of either component.
- dP_1 Induced power loss for blade elements.
- dP_2 Drag power loss for blade elements.
- dQ Torque on blade elements.
- r, R Radius of blade element, tip radius.
- s Solidity ($= Nc/2\pi r$) of either component.
- S suffix For single airscrew.
- dT Thrust on blade elements.
- u, v Components of interference velocity of front airscrew on back airscrew or vice versa (Fig. 1).
- V Forward speed (Fig. 1).
- W Resultant velocity at blade element (Fig. 1).
- W_0 Fig. 1.

12

List of Symbols—*continued*.

w_1	Interference velocity of either airscrew on itself (equation (1)).
\bar{w}_1	Equation (2).
y, z suffices	Denoting either front airscrew and back airscrew respectively, or vice versa (equation (17)).
0 suffices	Indicating limiting value for zero lift.
α	Blade incidence.
β	Fig. 1 ; equation (9).
γ	Fig. 1 ; equations (7) and (8).
ε	Zero lift angle ; equation (39).
ζ, ζ_0	Equations (70), (18).
η	Efficiency.
θ	Blade angle ; equation (39).
Θ	Equation (39).
κ	Tip loss factor ; equation (1). κ_0 is written for $\kappa(\phi_0)$.
λ_{yz}	Equation (22).
μ, μ_0 ν, ν_0	} Equations (69), (17).
ξ, ξ_0	Equations (70), (18).
ϕ, ϕ_0	Fig. 1. Equations (9), (10).
Ω	Angular velocity in radians per second.

Note. $O(\gamma^2)$. The notation used in equation (19) *etc.* The statement

$$F(\gamma) = F_1(\gamma) + O(\gamma^n)$$

implies that $F(\gamma)$ can be expanded in powers of γ in the form

$$F(\gamma) = f_0 + \gamma f_1 + \gamma^2 f_2 + \dots$$

and that

$$F_1(\gamma) = f_0 + \gamma f_1 + \gamma^2 f_2 + \dots + \gamma^{n-1} f_{n-1} .$$

REFERENCES

- | | | | |
|---|--------------------------|---------|---|
| 1 | Lock and Yeatman | | Tables for Use in an Improved Method of Airscrew Strip Theory Calculation. R. & M. 1674. October, 1934. |
| 2 | Lock | | A Graphical Method of Calculating the Performance of an Airscrew. R. & M. 1849. (R. & M. 1675 revised.) August, 1938. |
| 3 | Lock, Pankhurst and Conn | | Strip Theory Method of Calculation for Airscrews on High-speed Aeroplanes. R. & M. 2035. October, 1945. |
| 4 | Pankhurst and Fowler | | Calculations of the Performance of Two Airscrews for a High-speed Aeroplane. R. & M. 2021. April, 1941. |
| 5 | Lock | | Handbook of Aeronautics, 3rd Edition, Vol. III, 1938. Article "Airscrews," p. 177. |

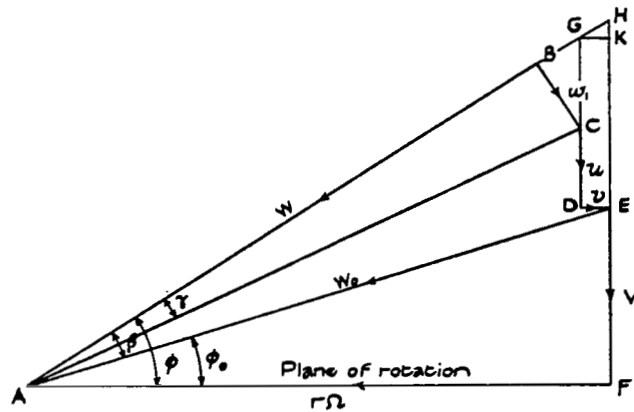


FIG. 1 (a). Either Airscrew.

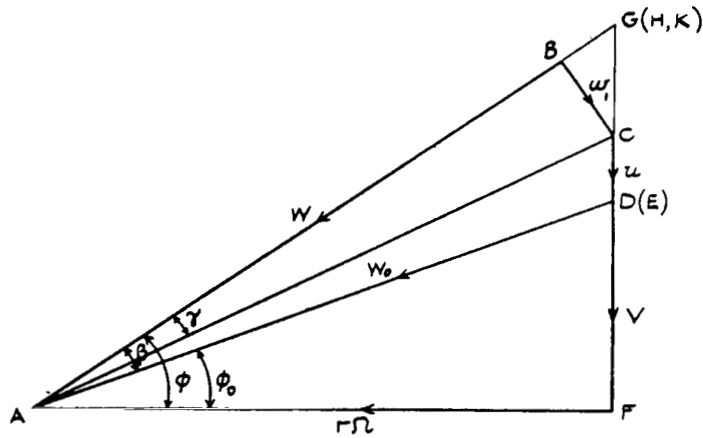


FIG. 1 (b). Front Airscrew.

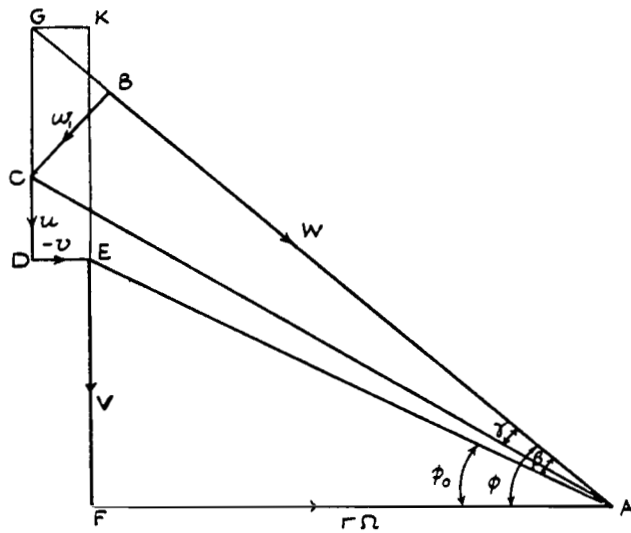


FIG. 1 (c). Back Airscrew.

FIG. 1. Interference Velocity Components for a Contra-rotating Pair of Airscrews.

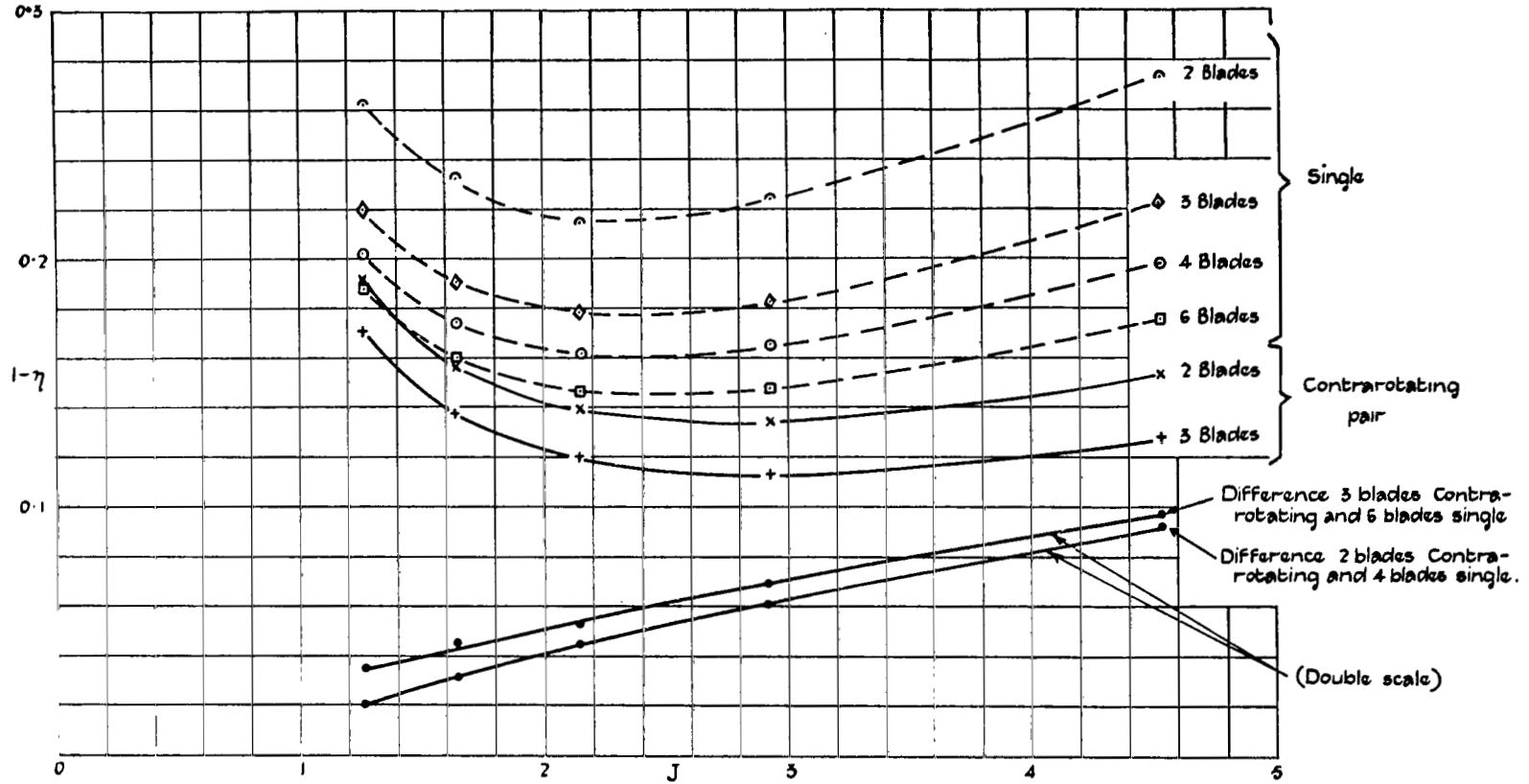


FIG. 2. Ideal Loss of Efficiency at Standard Radius 0.7, Plotted against J . All curves calculated for same values of s (0.09), C_L (0.56), C_D (0.017) (total solidity 0.18).

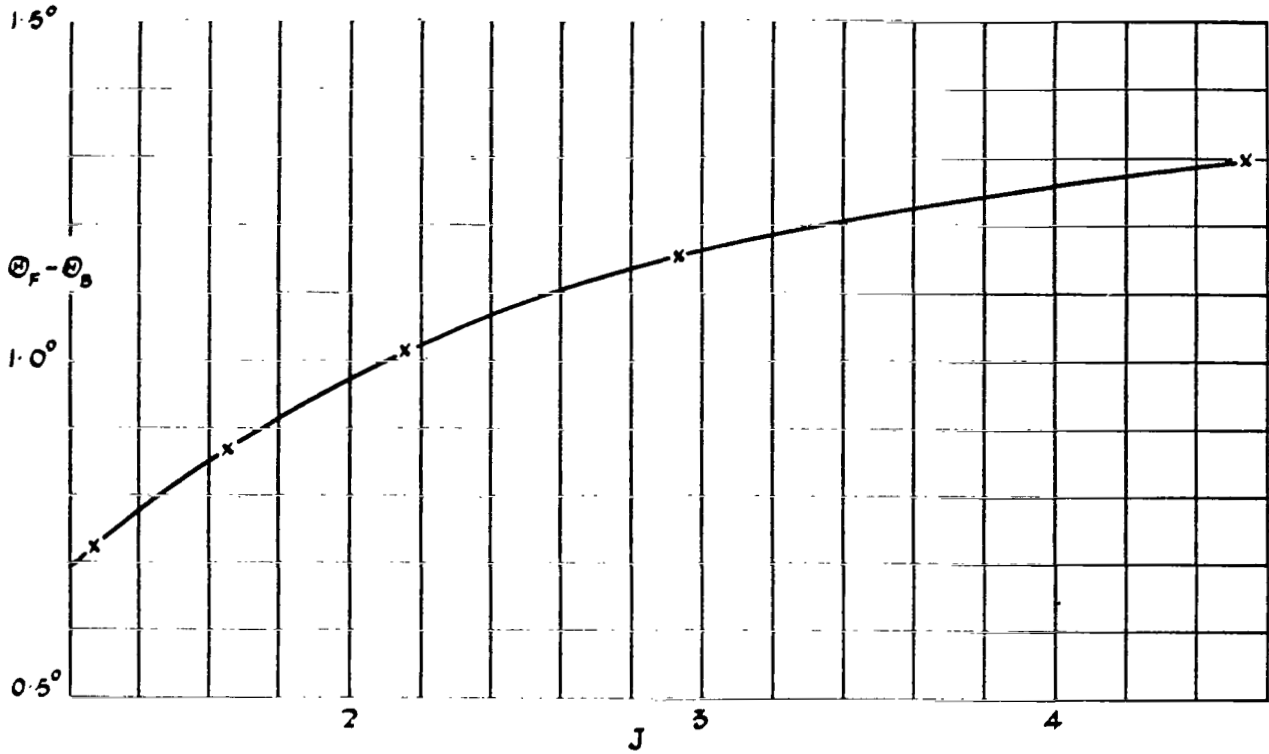


FIG. 3. Values of $(\theta_F - \theta_B)$ (independent of number of blades) Calculated for Same Conditions as Fig. 2 (for Equal Rotational Speed). The Curve also Represents the Difference of Blade Angles $(\theta_F - \theta_B)$ provided that the Zero Lift Angles are the Same for Both Airscrews.

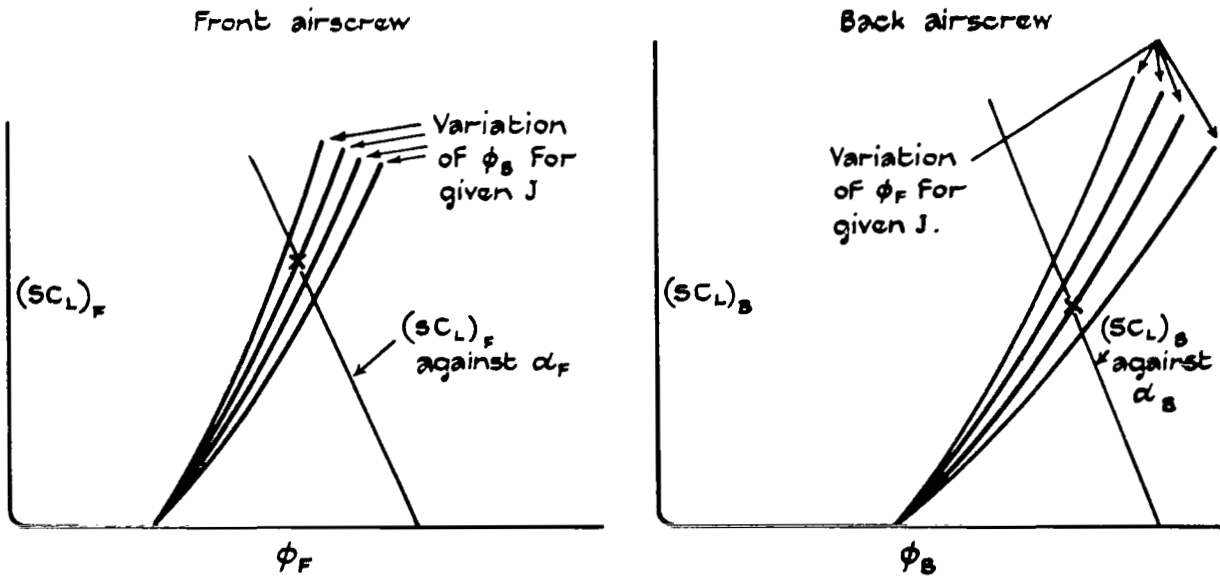


FIG. 4. Charts Analogous to Chart I of R. & M. 1849².

(76164) Wt. 10/7116 6/47 Hw. G.377/1.

APPENDIX C

INDEPENDENT DERIVATION OF LOCK'S TIP LOSS FACTOR FORMULA

In the text, χ_0 was found by making σ , or optimum planforms, the same between Lock and Theodorsen. Now, however, the induced angles β will be made the same between the two formulations.

The first thing will be to specialize Lock's theory to apply where the propellers are in the same plane. (The determination of χ_0 is the same whether they are or are not in the same plane, as was seen in the text.) This specialization makes the two equations for ζ_{0y} , between equations (28) and (29) in appendix B, become symmetric so that they are one

$$\zeta_0 = \chi_0 (\cos^2 \phi_0 - \sin^2 \phi_0) = r' \chi_0 \quad (C1)$$

Then the induced angle of attack, equation (B27), becomes

$$\beta = b(1 + \zeta_0)\sigma = b(1 + r'\chi_0)\sigma \quad (C2)$$

for either propeller, where

$$b = \frac{1}{4\chi_0 \sin \phi_0} \quad (C3)$$

from equation (B23).

Now β is the induced angle of attack at the propeller plane, not the far wake. The induced angle of attack from Theodorsen, therefore, must be multiplied by 1/2. Also, the displacement velocity w multiplied by $\cos \phi_0$ gives the velocity of the vortex sheet normal to itself. If this is divided by W_0 it is converted to an induced angle. Thus, the equating of the induced angle, between Lock and Theodorsen, yields

$$\frac{1}{2} \frac{w}{W_0} \cos \phi_0 = \beta \quad (C4)$$

with the right side given by equation (C2).

Next, Theodorsen's circulation function will be introduced, as in the text just before equation (13),

$$sC_L W_0 = \sigma W_0 = \frac{V}{\pi n dx} \bar{w} V K(x) \quad (C5)$$

or

$$\frac{\sigma}{w} = \frac{J}{\pi x} \sin \phi_0 K(x) \quad (C6)$$

where

$$\bar{w} = w/v \quad (C7)$$

Now equation (C4) can be written, by using equation (C2),

$$\frac{\frac{1}{2} \cos \phi_0}{w_0} = \frac{\beta}{w} = \frac{\beta}{v\bar{w}} = \frac{b(1 + r'\chi_0)}{v} \frac{\sigma}{\bar{w}} \quad (C8)$$

By using equation (C3), equation (C8) becomes

$$\frac{\frac{1}{2} \cos \phi_0}{w_0} = \frac{\frac{1}{4 \sin \phi_0} \left(\frac{1}{\chi_0} + r' \right)}{v} \frac{J}{\pi x} K(x) \sin \phi_0$$

Substituting $v/w_0 = \sin \phi_0$ (fig. 1 of app. B) and multiplying by $4 \sin \phi_0$ result in

$$\sin 2\phi_0 = \left(\frac{1}{\chi_0} + r' \right) \frac{J}{\pi x} K(x) \quad (C9)$$

Solving for χ_0 gives

$$\chi_0 = \frac{1}{\frac{\pi x}{JK(x)} \sin 2\phi_0 - r'} \quad (C10)$$

Now, the corresponding formula in the text is equation (17), which is

$$\chi_0 = \frac{1}{\frac{kp'}{q'\bar{w}s'} - r'} \quad (C11)$$

Compare equations (C10) and (C11), which should be identical. They will be identical if

$$\frac{kp'}{q'\bar{w}s'} \equiv \frac{\pi x}{JK(x)} \sin 2\phi_0 \quad (C12)$$

APPENDIX C

Substitute the following from equations (16) in the text, into equation (C12):

$$\left. \begin{aligned} p' &= \frac{1}{2} \phi_{q0} \cos \phi_0 = \frac{1}{2} \sin \phi_0 \cos \phi_0 \\ q' &= \frac{2}{4 \sin \phi_0} \\ s' &= \frac{J}{\pi x} K(x) \sin \phi_0 \end{aligned} \right\} (\ell = 0) \quad (C13)$$

Then the right side of equation (C12) is

$$\frac{\pi x}{JK(x) \sin \phi_0} \sin \phi_0 \sin 2\phi_0 = \frac{1}{s'} \sin \phi_0 \sin 2\phi_0 \quad (C14)$$

and the left side is

$$\begin{aligned} \frac{\frac{k}{w} \frac{1}{2} \sin \phi_0 \cos \phi_0}{\frac{2}{4 \sin \phi_0} s'} &= \frac{k}{w} \frac{1}{s'} 2 \sin \phi_0 \frac{1}{2} \sin \phi_0 \cos \phi_0 \\ &= \frac{k}{w} \frac{1}{2} \frac{\sin \phi_0}{s'} \sin 2\phi_0 \end{aligned} \quad (C15)$$

Equating equations (C14) and (C15) gives

$$\frac{1}{2} \frac{k}{w} = 1 \quad (C16)$$

which must be true in order for equations (C10) and (C11) to be the same. But equation (C16) is in fact true, as may be seen from equations (22) in the text.

Hence it is concluded that the two formulas, (C10) and (C11), are indeed equivalent, and it appears to be verified that the method given in the present paper for determining χ_0 , appendix D, is correct and consistent with Theodorsen and Lock.

APPENDIX D

CALCULATION OF χ_0 FOR DUAL-ROTATION PROPELLER AT A GIVEN VALUE FOR J

1. Choose a set of values of x corresponding to stations or sections on the propellers at various radii. These values of x might well be those found in figure 2. The entire calculation is performed for each value of x .

2. Calculate the advance angle ϕ_0 from

$$\phi_0 = 90^\circ - \tan^{-1} \left(\frac{\pi}{J} x \right)$$

3. For the values of x chosen in step 1, read a set of $K(x)$ from the circulation function curves (e.g., fig. 2) for the number of blades being considered (four front and four back for the purposes of this paper.)

4. Calculate p' , q' , r' , and s' from equations (16). Note that, since ℓ is taken to be zero in this calculation, $\phi_{q0} = \sin \phi_0$.

5. Calculate χ_0 from equation (17). (The value of k/\bar{w} was determined to be 2.0 in the discussion following equation (17). (See eqs. (22).)

APPENDIX E

OPTIMIZATION OF DUAL-ROTATION PROPELLER WITH DRAG CONSIDERED

1. A value for J and a value for C_p must be given to start.
2. Tabulate χ_0 from step 5 in appendix D.
3. Tabulate the preselected C_L , l , and α for each x . For instance, these might be for maximum lift-drag ratio all along the blade.
4. Calculate ϕ_{q0} from equation (9).
5. Calculate σ from equation (12). In this step, a trial value for k is needed. Equation (19) is an aid in guessing this.
6. Integrate dC_p/dx over the range of x , from body to tip, and compare the resulting C_p to the given C_p , which must match.

$$\frac{dC_p}{dx} = \frac{\pi^4}{2} (\sec^2 \phi_0) x^4 \sigma \phi_{q0} \quad (\text{for both propellers})$$

This equation can be derived from equation (8). Set $w^2 = r^2 \Omega^2 \sec^2 \phi_0$. Change r to xR and use $C_p \equiv \Omega Q / (\rho n^3 d^5)$.

7. Calculate

$$\frac{c}{d} = \frac{\pi}{B} \frac{x\sigma}{C_L}$$

8. Find β_F and β_B from equations (27).
9. Calculate the blade-angle distribution θ from equation (23).

$$\theta_F + (\text{Torsional deflection}) = \phi_0 + \beta_F + \alpha$$

$$\theta_B + (\text{Torsional deflection}) = \phi_0 + \beta_B + \alpha$$

Items 7 and 9 define the propeller.

APPENDIX F

CALCULATING PERFORMANCE OF GIVEN DUAL-ROTATION PROPELLER

AT OFF-DESIGN CONDITIONS

The problem may be stated as: given the propeller at some blade-angle setting and the value of J , determine the torque and thrust, or determine the power absorption and efficiency.

The existence of initial distributions of $(C_L)_F$ and $(C_L)_B$ and hence of σ_F and σ_B can be assumed. This may be a guess, or else they can be calculated immediately by assuming the induced angle of attack is zero.

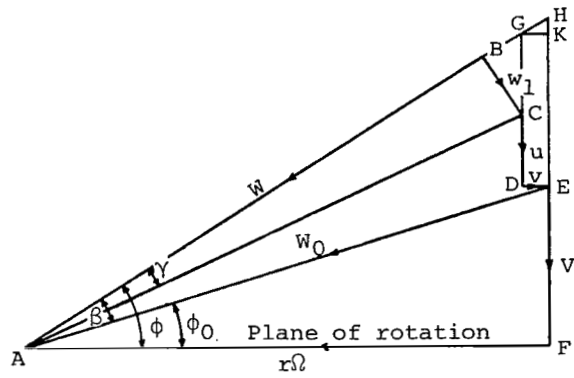
1. Follow the steps in appendix D to obtain the function χ_0 applicable to the given J .
2. Calculate ϕ_{q0} from equation (9) (the same as step 4 in app. E).
3. Tabulate or store airfoil data so that C_L and l can be found for any value of α . (Note that this is not the same kind of airfoil data as in step 3 of app. E, which is preselected airfoil data.)
4. Tabulate θ_F , θ_B , and s from propeller-geometry information and the given blade-angle setting.
5. Calculate β_F and β_B from equations (28). Initially, these might be set equal to zero.
6. Solve equation (29) for α_F and α_B .
7. Find new $(C_L)_F$ and $(C_L)_B$ from airfoil data using α_F and α_B from step 6. Also find new σ_F and σ_B .

After completing step 7, it is possible to return to step 5 and loop through to step 7 repeatedly until $(C_L)_F$ and $(C_L)_B$ converge on final values. At step 7 on the last loop, find l_F and l_B in addition to the lift coefficients. Then step 6 in appendix E shows how to get the power input. The efficiency is found as in equation (18), but by using equation (6) instead of equation (2). Note that in place of σ there are σ_F and σ_B . Therefore, the power formula in step 6, appendix E, has to be appropriately modified. The same applies to equation (6) in the efficiency calculation. This would conclude the calculation if arbitrary propeller theory were not to be added.

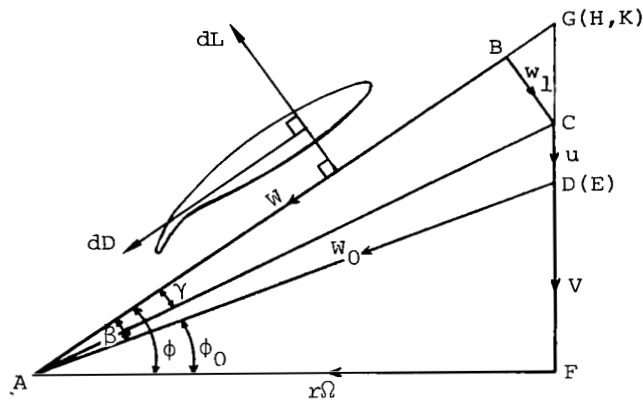
If arbitrary theory is to be introduced, the return to step 5, after completing step 7 on the last loop, would call for arbitrary propeller theory rather than equations (28). More specifically, the circulation can be easily found from $(C_L)_F$ and $(C_L)_B$, which are found in step 7. From the circulation, the single-rotation part of the induced angle of attack γ_y can be found, by arbitrary propeller theory, so that β_y now contains arbitrary propeller theory. The tip loss factor χ_0 is no longer used. The loop continues on to step 7. This should produce a rigorous lifting-line performance calculation, but the introduction of arbitrary propeller theory has to be regarded as a considerable escalation of computational effort.

REFERENCES

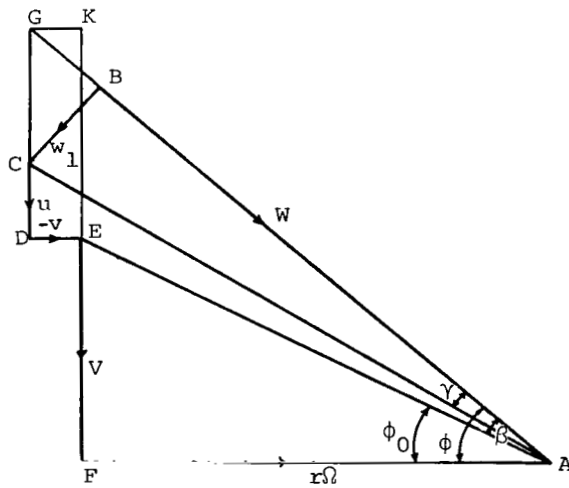
1. Crigler, John L.: Application of Theodorsen's Theory to Propeller Design. NACA Rep. 924, 1949. (Supersedes NACA RM L8F30.)
2. Theodorsen, Theodore: The Theory of Propellers. II - Method for Calculating the Axial Interference Velocity. NACA Rep. 776, 1944. (Supersedes NACA ACR L4I19.)
3. Theodorsen, Theodore: Theory of Propellers. McGraw-Hill Book Co., Inc., 1948.
4. Reissner, H.: On the Relation Between Thrust and Torque Distribution and the Dimensions and the Arrangement of Propeller-Blades. Phil. Mag., ser. 7, vol. 24, no. 163, Nov. 1937, pp. 745-771.
5. Goldstein, Sydney: On the Vortex Theory of Screw Propellers. Proc. Roy. Soc. (London), ser. A, vol. 123, no. 792, Apr. 6, 1929, pp. 440-465.
6. Lock, C. N. H.; and Yeatman, D.: Tables for Use in an Improved Method of Airscrew Strip Theory Calculation. R. & M. No. 1674, British A.R.C., 1935.
7. Theodorsen, Theodore: The Theory of Propellers. I - Determination of the Circulation Function and the Mass Coefficient for Dual-Rotating Propellers. NACA Rep. 775, 1944. (Supersedes NACA ACR L4H03.)
8. Lock, C. N. H.: Interference Velocity for a Close Pair of Contra-Rotating Airscrews. R. & M. No. 2084, British A.R.C., July 22, 1941.
9. Durand, William Frederick, ed.: Aerodynamic Theory. Volume IV. Julius Springer (Berlin), 1935, pp. 251-254.
10. Margenau, Henry; and Murphy, George Moseley: The Mathematics of Physics and Chemistry. D. Van Nostrand Co., Inc., c.1943.



(a) Either airscrew.



(b) Front airscrew.



(c) Back airscrew.

Figure 1.- Interference velocity components for pair of dual-rotation propellers.

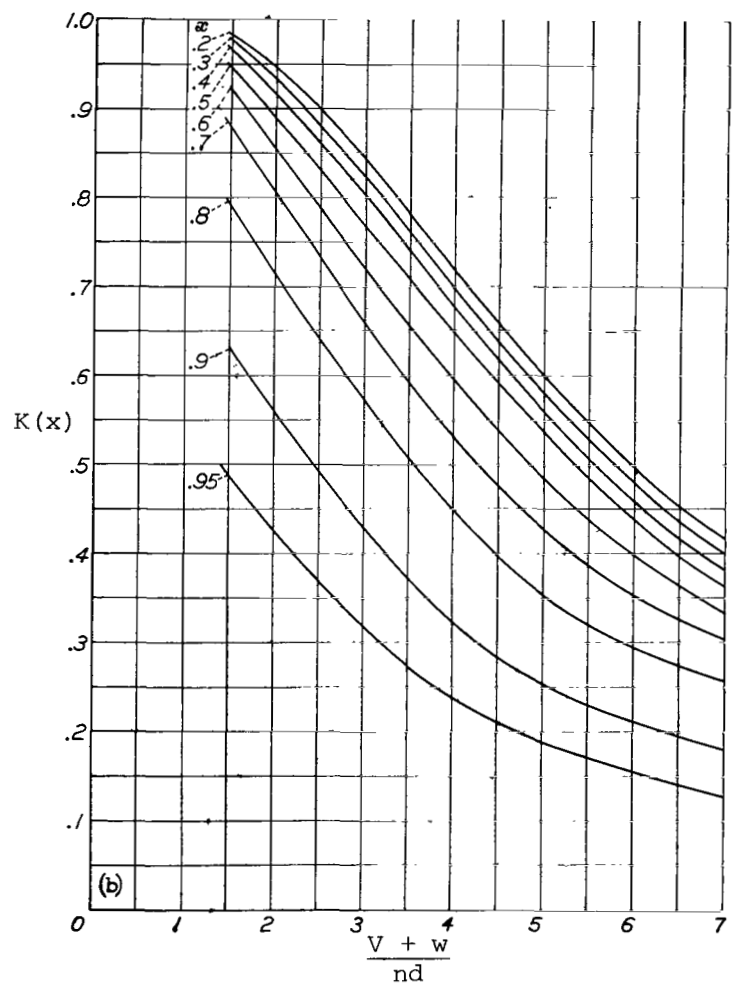


Figure 2.- Circulation function $K(x)$ for dual-rotation propellers; four blades front and four blades back (ref. 1).

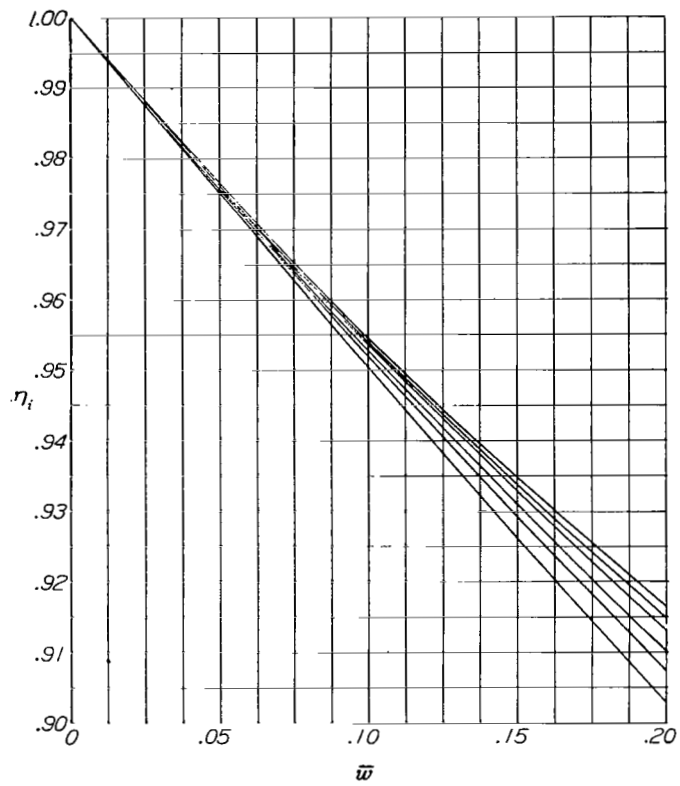


Figure 3.- Propeller induced efficiency plotted against \bar{w} (ref. 1).

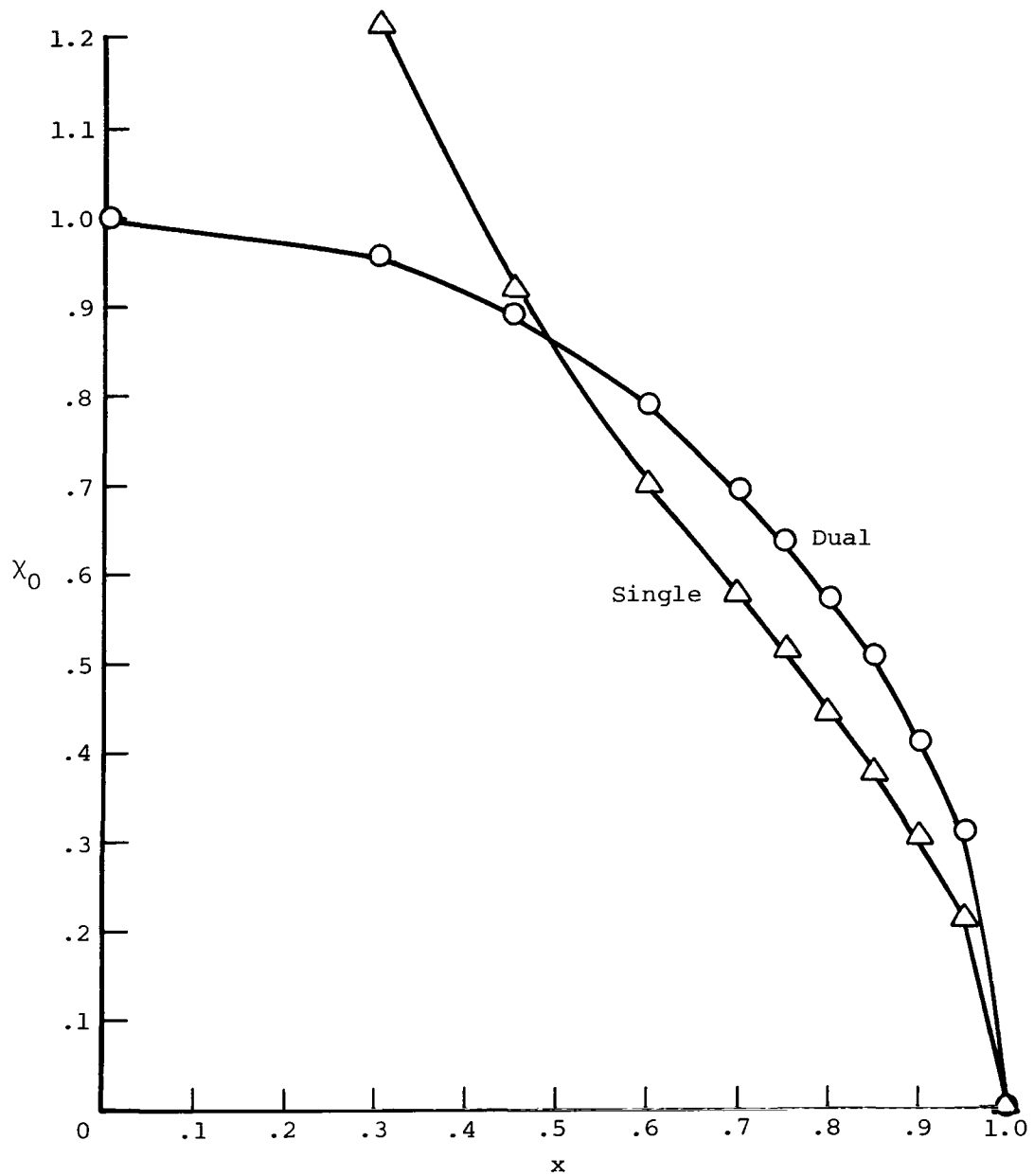


Figure 4.- Tip loss factors for single- and dual-rotation propellers plotted against x ; $J = 5.1693$, four blades single, eight blades dual.

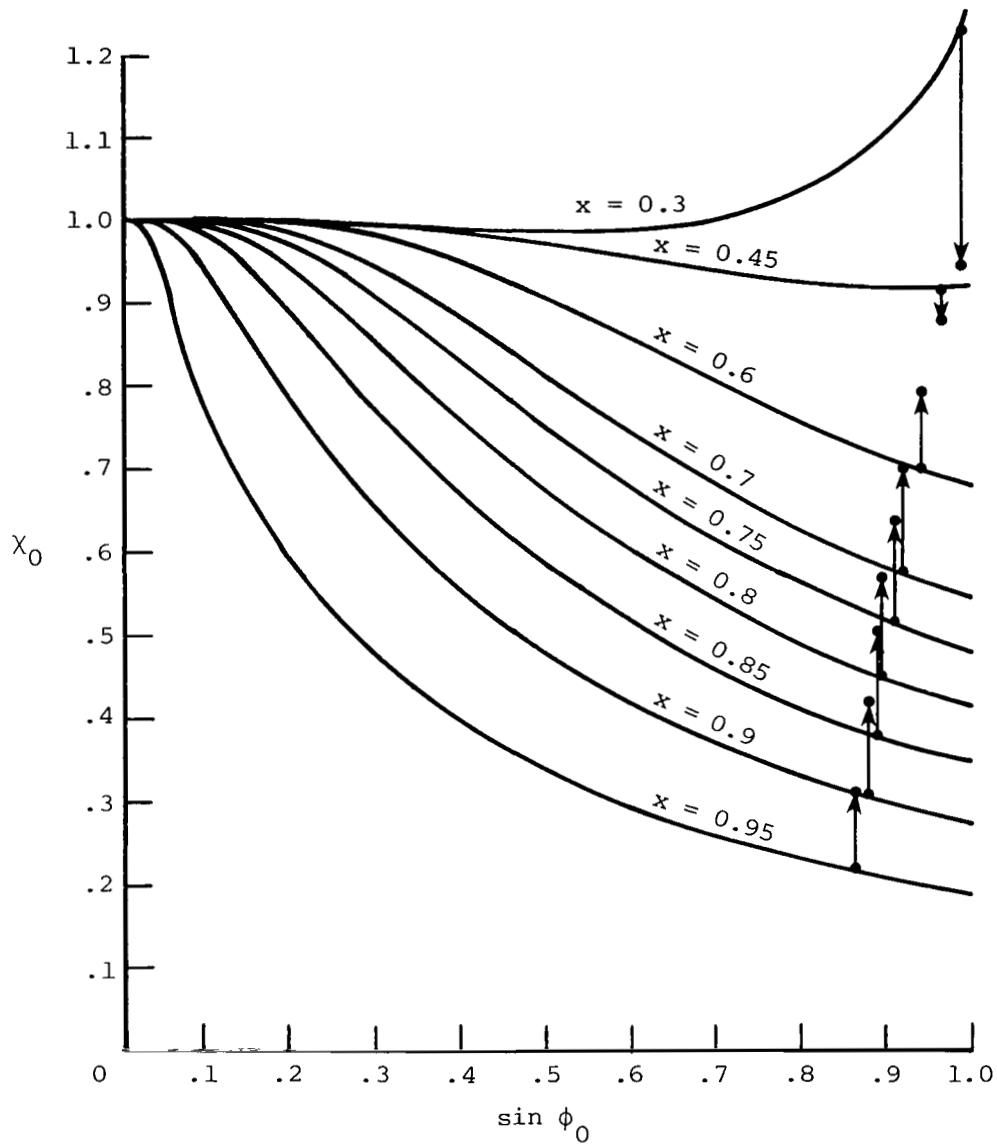


Figure 5.- Typical presentation of X_0 for single rotation for four blades. Arrows show how typical points on curves shift for dual rotation of eight blades (four front and four back). Shifted points shown are for $J = 5.1693$. (See ref. 6.)

1. Report No. NASA TP-1948		2. Government Accession No.		3. Recipient's Catalog No.	
4. Title and Subtitle OPTIMIZATION AND PERFORMANCE CALCULATION OF DUAL-ROTATION PROPELLERS				5. Report Date December 1981	
7. Author(s) Robert E. Davidson				6. Performing Organization Code 505-31-33-08	
9. Performing Organization Name and Address NASA Langley Research Center Hampton, VA 23665				8. Performing Organization Report No. L-14678	
12. Sponsoring Agency Name and Address National Aeronautics and Space Administration Washington, DC 20546				10. Work Unit No.	
15. Supplementary Notes				11. Contract or Grant No.	
16. Abstract An analysis is given which enables the design of dual-rotation propellers. It relies on the use of a new tip loss factor deduced from T. Theodorsen's measurements coupled with the general methodology of C. N. H. Lock. In addition, it includes the effect of drag in optimizing. Some values for the new tip loss factor are calculated for one advance ratio.				13. Type of Report and Period Covered Technical Paper	
17. Key Words (Suggested by Author(s)) Propeller blades Performance Dual rotation calculation Optimization Airfoil drag contrarotating				14. Sponsoring Agency Code	
18. Distribution Statement Unclassified - Unlimited Subject Category 01					
19. Security Classif. (of this report) Unclassified		20. Security Classif. (of this page) Unclassified		21. No. of Pages 46	22. Price A03

National Aeronautics and
Space Administration

Washington, D.C.
20546

Official Business
Penalty for Private Use, \$300

THIRD-CLASS BULK RATE

Postage and Fees Paid
National Aeronautics and
Space Administration
NASA-451



3 1 U.A. 120381 30090305
DEPT OF THE AIR FORCE
AF WEAPONS LABORATORY
ATTN: TECHNICAL LIBRARY (JUL)
CITIZENSHIP AND 5/11/7

NASA

POSTMASTER: If Undeliverable (Section 158
Postal Manual) Do Not Return
